JOURNAL OF SOLID STATE CHEMISTRY **128,** 130–136 (1997)
ARTICLE NO. SC967186

# Ordering of Anionic Vacancies in the $BaCoO_{2.94}$ Hexagonal Related Perovskite

A. Varela,* M. Parras,* K. Boulahya,* and J. M. González-Calbet*,†,[1]

* *Departamento Química Inorgánica, Facultad Químicas, Universidad Complutense, 28040 Madrid, Spain; and*
† *Instituto de Magnetismo Aplicado (RENFE-UCM), Apdo. 155, 28230 Las Rozas, Madrid, Spain*

Received July 29, 1996; in revised form October 1, 1996; accepted October 14, 1996

**An electron diffraction and high-resolution electron microscopy study shows that oxygen vacancies in $BaCoO_{2.94}$ lead to a threefold superstructure along the $(11\bar{2}0)_{2H}$ direction, the … hhh … hexagonal sequence characteristic of the 2H type being maintained. According to compositional and structural data, the most probable structural model should be formed by three $AO_3$ layers intergrowing with one $AO_{2.67}$ layer along the *c*-axis. In such oxygen-deficient layers, one of each six oxygen atoms in every oxygen row is removed, leading to the observed superstructure.** © 1997 Academic Press

## 1. INTRODUCTION

In previous papers, we have reported the microstructural characterization of oxygen-deficient $ABO_{3-y}$ hexagonal related perovskites, showing the different behavior of $BaMnO_{3-y}$ (1, 2) and $BaFeO_{3-y}$ (3) systems. The accommodation of oxygen vacancies is closely related to the *B* cation size and/or the different stable environments for *B* cations occupying the cationic sublattice.

Considering the 2H related materials, one of the systems less studied is the Ba–Co–O. In fact, only few results have been published concerning the $BaCoO_{3-y}$ phases. Stoichiometric $BaCoO_3$ have been reported by Taguchi *et al.* (4) to be isostructural to $BaNiO_3$ (5). On the other hand, $BaCoO_2$ was described by Spitsbergen (6). According to X-ray diffraction (XRD) data, it seems to be isostructural to $BaZnO_2$, however, detailed structural features were not shown. Intermediate compositions (with $Co^{3+}/Co^{4+}$) have been reported by Zanne *et al.* (7). These authors propose a phase diagram with six different phases, characterized by X-ray diffraction, as a function of the oxygen content. However, the relationship between oxygen nonstoichiometry, vacancy ordering, and microstructure is not fully understood.

A microstructural characterization of the 12H $BaCoO_{2.6}$ has been carried out by Jacobson and Hutchison (8), by means of HREM and profile analysis of powder diffraction data, showing that its structure can be described as a … $(cc'chhh)_2$ … sequence, where c and h are cubic and hexagonal $BaO_3$ layers, respectively, and c′ stands for $BaO_2$ layers. The replacement of $BaO_3$ by $BaO_2$ layers leads to tetrahedral coordination for cobalt cations.

Recently (9), we have reported a new phase in this system, $BaCoO_{2.74}$, which is a 5H polytype. The structure is based on a 5-layer stacking sequence … ccchh … where one $BaO_3$ layer is replaced by one $BaO_2$ layer, per unit cell, leading to two-fifths of the Co atoms in tetrahedral coordination.

In this paper, we report the study of $BaCoO_{2.94}$. For highly oxidized $BaCoO_{3-y}$ materials, Zanne *et al.* (7) reported that, according to XRD data, the 2H structural type is preserved along $BaCoO_3$–$BaCoO_{2.85}$. Our study, by means of selected area electron diffraction (SAED) and high-resolution electron microscopy, shows a somewhat different situation.

## 2. EXPERIMENTAL

The $BaCoO_{2.94}$ sample was obtained by heating stoichiometric amounts of $BaCO_3$ and $Co_3O_4$ at 700°C for 14 h. The stoichiometric $BaCoO_3$ material, which was used to compare diffraction data, was prepared by heating the starting material at 900°C under 200 bar $O_2$ for 24 h.

In order to prove the lack of carbon, elemental analysis was performed on a Perkin–Elmer 2400 CHN analyzer, no more than 1% of C being detected. The 1:1 cationic ratio was confirmed by inductive coupling plasma (ICP).

The oxygen content was determined by thermogravimetric analysis developed on the basis of a CAHN D-200 electrobalance. Samples were reduced under 300 mbar $H_2$/200 mbar He at 800°C. Since the final product of the reduction process was always the same mixture of Co and BaO, the oxygen content was established

[1] To whom correspondence should be addressed.



0022-4596/97 $25.00

from the weight difference between the starting and final products.

Powder XRD was performed on a SIEMENS D5000 diffractometer with a graphite monochromator and using Cu$K\alpha$ radiation. Selected area electron diffraction (SAED) and electron microscopy were carried out on a JEOL 2000FX electron microscope. High-resolution electron microscopy (HREM) was performed on a JEOL 4000 EX electron microscope.

## 3. RESULTS AND DISCUSSION

Powder XRD patterns corresponding to both $BaCoO_3$ and $BaCoO_{2.94}$ samples are shown in Figs. 1a and 1b, respectively. All diffraction maxima corresponding to the $BaCoO_3$ sample can be indexed on the basis of the 2H unit cell characteristic of $BaNiO_3$ (5), with parameters $a = 0.563$ and $c = 0.476$ nm, $P63/mmc$ space group, in good agreement with Taguchi *et al.* (4).

The $BaCoO_{2.94}$ XRD pattern is quite similar to that shown by $BaCoO_3$. In fact, the most intense reflexions (marked with an asterisk) correspond to a 2H hexagonal unit cell, but other less intense superstructure reflexions appear. In order to investigate the origin of such extra reflexions, a SAED and HREM study was performed.

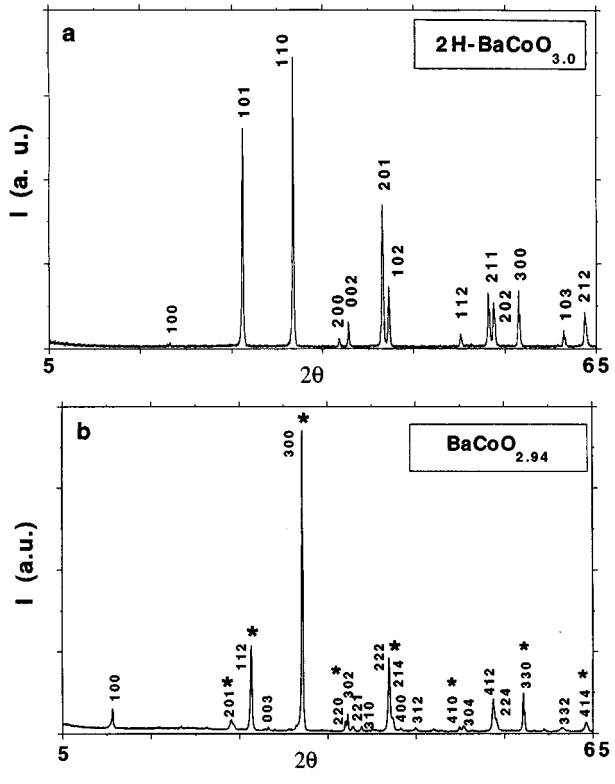


**FIG. 1.** Powder X-ray diffraction pattern of (a) $BaCoO_3$ (2H structural type) and (b) $BaCoO_{2.94}$.

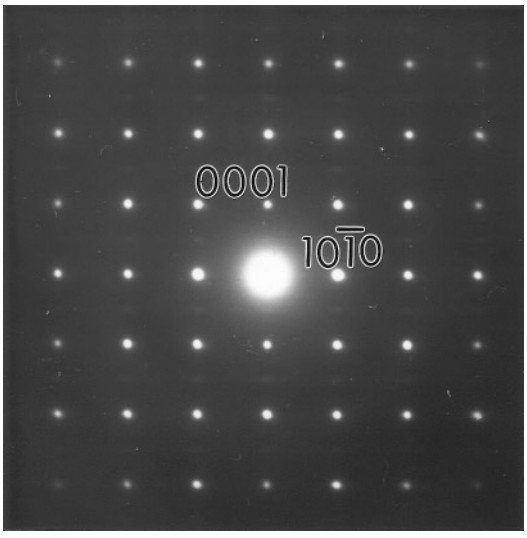


**FIG. 2.** SAED pattern of $BaCoO_{2.94}$ along the $[01\bar{1}0]_{2H}$ zone axis.

Figure 2 shows the SAED pattern of the $BaCoO_{2.94}$ material along the $[01\bar{1}0]_{2H}$ zone axis. All diffraction spots can be indexed on the basis of a 2H unit cell, but the presence of diffuse streaking parallel to the $a^*$ direction and doubling $c$-axis suggests the existence of some disorder and possibly larger periodicity for the $c$-axis.

By tilting around the $c^*$-axis, the SAED pattern along $[1\bar{1}00]_{2H}$ is obtained (Fig. 3a). The strongest diffraction maxima corresponds to the 2H subcell, but also a threefold superstructure along $(11\bar{2}0)_{2H}$ is observed. Once again, weak streaking parallel to the $(11\bar{2}0)_{2H^*}$ direction and doubling $c^*$-axis appears. The corresponding high resolution electron micrograph is shown in Fig. 3b. An apparently ordered crystal is seen with fringes of $d = 0.84$ nm, confirming the threefold superlattice along $(11\bar{2}0)_{2H}$. Although small variations in the contrast are detected following the $(11\bar{2}0)_{2H}$ direction, not many conclusions can be extracted from the origin of the streaking along such a direction. Unfortunately, the synthesis temperature leads to relatively thick crystals with only appropriate thickness for high-resolution conditions when seen along the $c$-axis.

Figure 4a shows the SAED pattern along the $[0001]_{2H}$ zone axis. Besides the strong reflections characteristic of the 2H subcell, threefold superstructure spots are seen along $[11\bar{2}0]^*$ and equivalent directions. Figure 4b shows the corresponding high resolution image. The three $(11\bar{2}0)_{2H}$ equivalent directions clearly show the threefold superlattice.

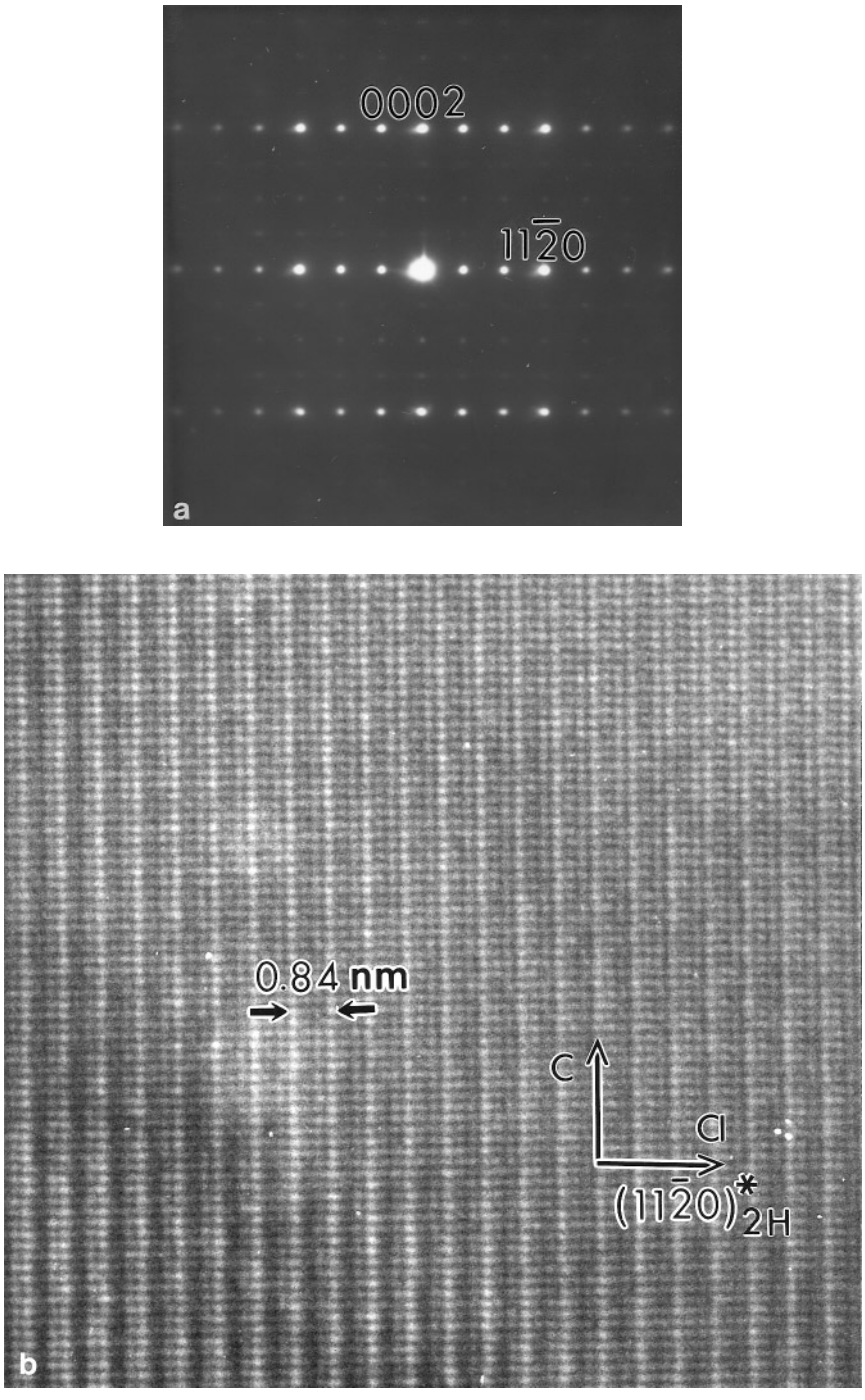


**FIG. 3.** (a) SAED pattern of $BaCoO_{2.94}$ along the $[1\bar{1}00]_{2H}$ zone axis. (b) Corresponding HREM.

From the ensemble of these results, the following relationship between the 2H-type and $BaCoO_{2.94}$ hexagonal reciprocal cells can be established:

$$a^* = 1/3[110]^*_{2H}$$

$$b^* = 1/3[\bar{1}20]^*_{2H}$$

$$c^* = 1/2[001]^*_{2H}$$

$$\begin{bmatrix} a \\ b \\ c \end{bmatrix}^* = \begin{bmatrix} 1/3 & 1/3 & 0 \\ \bar{1}/3 & 2/3 & 0 \\ 0 & 0 & 1/2 \end{bmatrix} \begin{bmatrix} a \\ b \\ c \end{bmatrix}^*_{2H}.$$

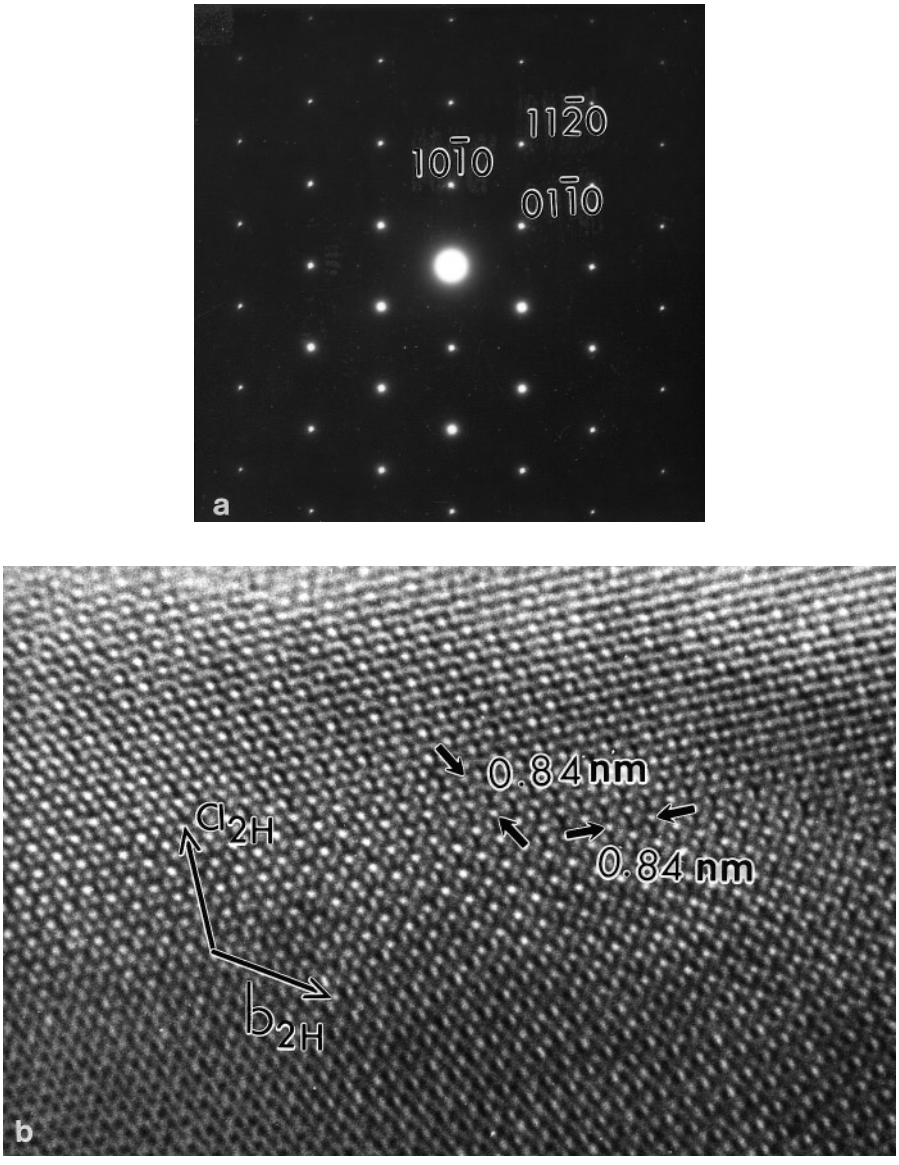


**FIG. 4.** (a) SAED pattern of $BaCoO_{2.94}$ along the $[0001]_{2H}$ zone axis. (b) Corresponding HREM.

The relationship between both direct cells is

$$\begin{bmatrix} a \\ b \\ c \end{bmatrix} = \begin{bmatrix} 2 & 1 & 0 \\ \bar{1} & 1 & 0 \\ 0 & 0 & 2 \end{bmatrix} \begin{bmatrix} a \\ b \\ c \end{bmatrix}_{2H},$$

leading to the following relationship between unit cell parameters:

$$\begin{aligned} \vec{\mathbf{a}} &= 2\overrightarrow{\mathbf{a}_{2H}} + \overrightarrow{\mathbf{b}_{2H}} & a &= \sqrt{3}a_{2H} \\ \vec{\mathbf{b}} &= \overrightarrow{\mathbf{b}_{2H}} - \overrightarrow{\mathbf{a}_{2H}} & b &= \sqrt{3}a_{2H} \\ \vec{\mathbf{c}} &= 2\overrightarrow{\mathbf{c}_{2H}} & c &= 2c_{2H}. \end{aligned}$$

According to these results we can conclude that $BaCoO_{2.94}$ shows a hexagonal unit cell with parameters $a \approx 0.969$ nm and $c \approx 0.48$ nm. With this unit cell, all X-ray diffraction maxima corresponding to $BaCoO_{2.94}$ sample, can be indexed as shown in Fig. 1b.

Figure 5 schematizes the (0001) plane, corresponding to the $BaCoO_{2.94}$ sample, showing an increasing of $\sqrt{3}$ times in the $a_{2H}$, $b_{2H}$ parameters and a rotation of the 2H axes by 30°.

A threefold superstructure in $ABO_3$ related materials following the $(11\bar{2}0)_{2H}$ direction has been previously reported by Poeppelmeier *et al.* (10) for $Ba_3W_2O_9$. This ordering is due to the spatial arrangement between chains constituted by face-shared octahedra having pairs of

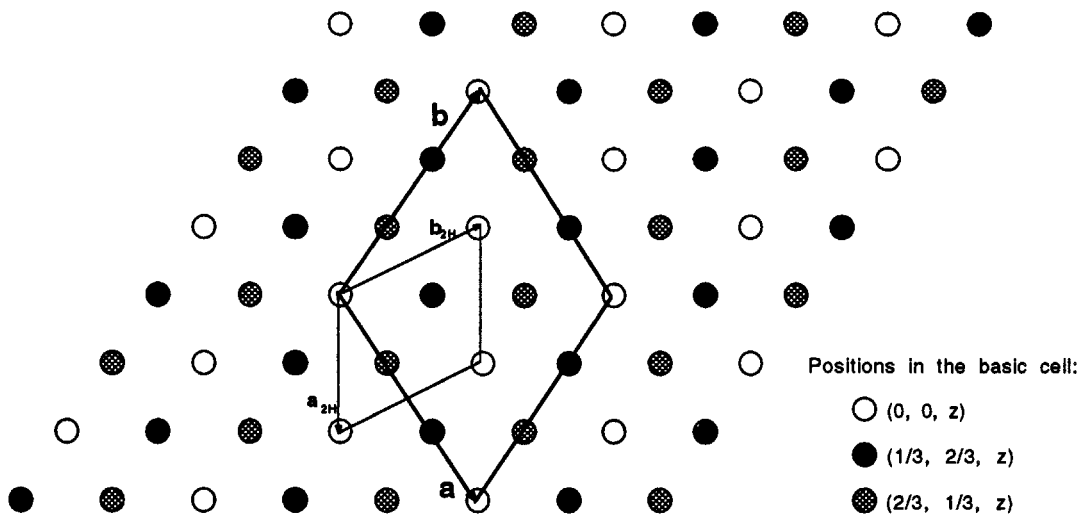


**FIG. 5.** Schematic representation of the $BaCoO_{2.94}$ structure projected along [0001]. $a_{2H}$ and $b_{2H}$ represent the 2H parameters; $a$ and $b$ represent the superstructure cell parameters. For simplicity, only Ba atoms are shown.

W atoms alternating with vacancies. Such an arrangement gives rise to a lattice constant expanded by the factor $\sqrt{3}$ and to a rotation of the reference axes by 30°. More recently, Spanchenko *et al.* (11) have reported a similar superstructure along the *ab*-plane for $Ba_8Ta_4Ti_3O_{24}$, once again as a consequence of *B* cationic vacancy ordering.

Moreover, it is worth mentioning that Candela *et al.* (12) reported the existence of a phase with composition $Ba_3B_2CO_{9-x}$ ($B$ = Co or Ni) showing the same structural features than $BaCoO_{2.94}$, probably due to some ordering between the *B* cations and some carbonate groups. As observed by elemental analysis, only less than 1% of carbon was detected in the sample. In any case, to be sure, a new sample was prepared from $BaO_2$ and $Co_3O_4$, the same XRD and SAED patterns being obtained. Therefore, the presence of C as a member of the structural building in our sample can be discarded.

Taking into account that carbon is not in the structure and considering that the Ba:Co ratio in our sample is, according to ICP data, 1:1, the ordering of oxygen vacancies must be responsible for the superstructure observed along the $(11\bar{2}0)_{2H}$ direction.

The first question concerning the introduction of anionic vacancies is if such a reduction process is accompanied of a modification of the … hhh … sequence by introduction of cubic layers. As previously reported in the $BaMnO_{3-y}$ related system (1, 2), the oxygen deficiency is accommodated by introduction of $BaO_{2.5}$ cubic layers in the hexagonal close packing of 2H-$BaMnO_3$. The SAED patterns along $[01\bar{1}0]_{2H}$ in $BaMnO_{3-y}$ samples clearly show that the basic 2H subcell is not maintained. However, the SAED pattern along such a projection in $BaCoO_{2.94}$ indicates that the hexagonal packing is preserved.

By keeping such a hexagonal stacking sequence, the problem now is to determine the vacancy ordering leading to a threefold superstructure along $(11\bar{2}0)_{2H}$. Only two models seem to be possible. The first one is shown in Fig. 6 where two each six oxygen atoms are eliminated following every oxygen row. A small rearrangement of the oxygen atoms leads to a tetrahedral environment for Co (two per unit cell). The composition corresponding to such a layer is $A_3O_7$ ($AO_{2.33}$), seven $AO_3$ layers, and one $AO_{2.33}$ layer being necessary per unit cell to get an anionic composition close to the experimental one. Such a model leads to a fourfold superstructure along the *c*-axis, contradictory to the experimental fact obtained by electron diffraction.

The second possibility considers a lower number of oxygen vacancies per layer. As can be seen in Fig. 7, only one each six oxygen atoms every oxygen row is now removed, leading to square pyramidal coordination for some Co atoms (two per unit cell). The composition corresponding to the oxygen deficient layer is $AO_{2.67}$, three more $AO_3$ layers being now necessary per unit cell to get an anionic composition ($AO_{2.92}$) close to the experimental one.

Considering the information obtained by electron diffraction, only the second model is plausible since, as shown in Figs. 2 and 3, the *c*-axis is doubled, while only a fourfold superstructure would be consistent with the first one. Although $Co^{4+}$ and $Co^{3+}$ are usually octahedral and tetrahedrally coordinated, some materials with Co in square pyramidal coordination have been previously reported. This is the case for $YBa(Co_{2-x}B_x)O_5$ ($B$ = Cu, Fe) where double layers of $Co(B)O_5$ pyramids sharing corners are separated by yttrium layers (13–15). Moreover, a 2H-$Sr_2Co_2O_5$ related perovskite has been described (16) where the vacancy ordering seems to be consistent with a

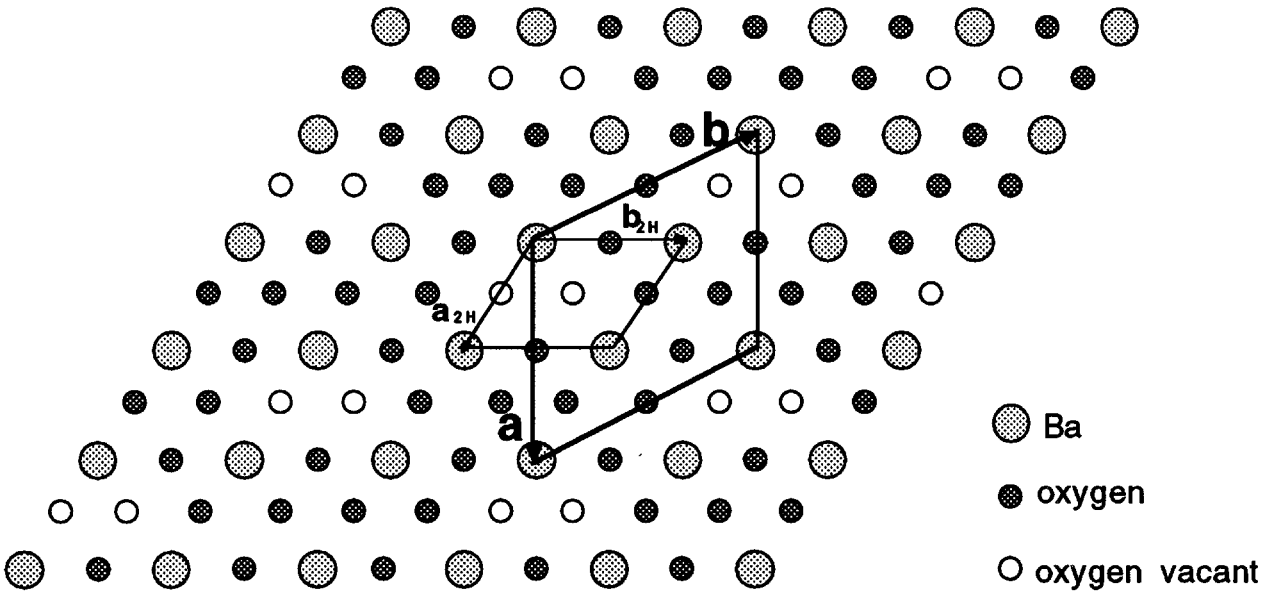


**FIG. 6.** Schematic representation of a possible layer $AO_{2.33}$ when two of each six oxygen atoms are removed from every oxygen row.

intermediate spin for $Co^{3+}$ leading to pyramidal and square planar coordination.

If the model shown in Fig. 7, is the correct one, there is still a small discrepance between the experimental and calculated oxygen content. However, it is worth recalling that some streaking appears along both *a*- and *b*-axes, probably due to an oxygen excess avoiding complete order of polyhedra in the *ab*-plane. In fact, the difference between the experimental and the theoretical composition leads to a change of about 6% square pyramids into octahedra along the crystal, probably explaining the described disorder.

As previously mentioned, such a superstructure use to be consistent with some ordering of the cationic vacancies (10, 11). However, as far as we know, Gai *et al.* (17) reported that, when heated at 1400°C, 9H-$BaIrO_3$ becomes orthorhombic, with the *a*-axis doubled with respect to the

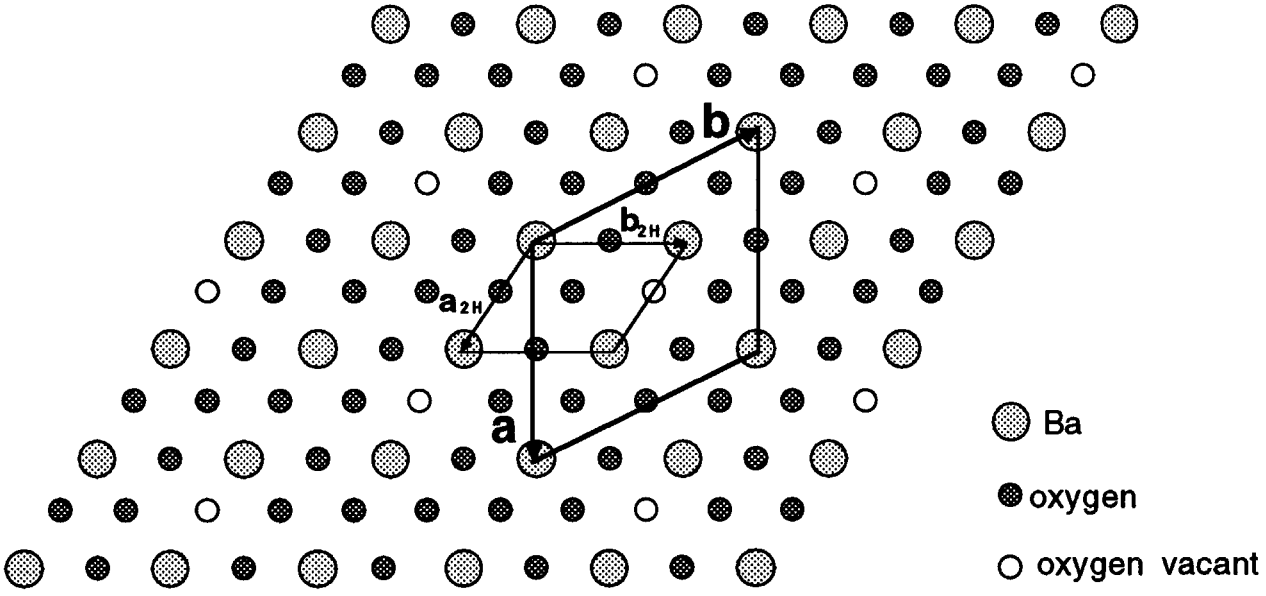


**FIG. 7.** Schematic representation of a possible layer $AO_{2.67}$ when one of each six oxygen atoms is removed from every oxygen row.

hexagonal 9H type. Such an ordering, according to the authors, could be a consequence of some $BaIrO_3$ reduction.

In previous papers, we have shown that oxygen vacancies in $BaMO_{3-y}$ hexagonal related perovskites ($M$ = Fe, Mn) are accommodated either at random ($BaFeO_{3-y}$) or leading to the formation of $BaO_{2.5}$ cubic layers ($BaMnO_{3-y}$) and, as a consequence, to new superstructures along the $c_{2H}$-axis. For instance, in the $BaFeO_{3-y}$ system the … hcchcc … stacking sequence characteristic of the 6H structural type, is preserved along ($0.20 < y < 0.25$) (3), the oxygen vacancies being at random in both c and h layers.

A somewhat different situation is observed in the $BaMnO_{3-y}$ system where every structural type shows a given composition, the accommodation of oxygen vacancies being related to the introduction of $BaO_{2.5}$ cubic layers. For comparison, note that in $BaMnO_{2.928}$ sample, showing an oxygen composition close to $BaCoO_{2.94}$, the small fraction of anionic vacancies is accommodated by means of the formation of three cubic layers per unit cell, leading to the 21R structural type with a stacking sequence … $(chhhhhh)_3$ … (2). In both systems the reduction process modifies the stacking sequence along $c$, but no additional ordering is detected along the $ab$-plane.

According to the above results, it is clear that $BaCoO_{3-y}$ shows a different behavior: the reduction process of the stoichiometric material, 2H-$BaCoO_3$, does not imply the formation of cubic layers. Even for a concentration of anionic vacancies as high as 7.3% per unit formula, i.e., $BaCoO_{2.78}$, the … hhh … stacking sequence is maintained (18). Only for more reduced materials (8, 9), structural types with alternating hexagonal and cubic layers are obtained.

Besides, in the $BaCoO_{3-y}$ system, only a small fraction of oxygen vacancies leads to ordering along the basal plane. This is the case for $BaCoO_{2.94}$ where a threefold superlattice along $(11\bar{2}0)_{2H}$ and equivalent directions implies ordering along the $ab$-plane. Evenmore, such a behavior could also be characteristic of the $BaNiO_{3-y}$ system, since $BaNiO_2$ (19) keeps the hexagonal close packing corresponding to the 2H-$BaNiO_3$ type although the environment for $Ni^{2+}$ in the first one is square planar. In fact, preliminary results in intermediate compositions support this behavior.

Considering that, in all cases, the reduction process is accompanied of a decreasing of the coordination index of $B$ cations leading to similar environment polyhedra, the difference observed in the final stacking sequence can only be due to the different characteristics of the atoms occupying the $B$ positions. For either Mn or Fe, the ionic size corresponding to $Mn^{3+}$ or $Fe^{3+}$ ($^{VI}r^{3+}_{Mn} = 0.64$ Å; $^{VI}r^{3+}_{Fe} = 0.64$ Å) (20) is high enough with respect to $Mn^{4+}$ or $Fe^{4+}$ ($^{VI}r^{4+}_{Mn} = 0.53$ Å; $^{VI}r^{4+}_{Fe} = 0.58$ Å) to introduce cubic layers in the hexagonal stacking sequence since the oxygen content decreases. Thus, the polyhedra share corners and $B$ cations increase their distance, decreasing the repulsions between them. For either Co or Ni, the trivalent ionic size ($^{VI}r^{3+}_{Co} = 0.54$ Å; $^{VI}r^{3+}_{Ni} = 0.56$ Å) is similar to that of $Mn^{4+}$, therefore, the hexagonal packing of $BaO_{3-y}$ layers does not change in the $BaCoO_{3-y}$ system up to a high vacant anionic concentration ($BaCoO_{2.74}$, i.e., 8.7% of anionic vacancies per unit cell) or is even preserved up to total reduction of $B^{4+}$ cations, as in $BaNiO_2$.

The magnetic study of cobalt should introduce more light on the behavior of this system due to its great ability of adopt intermediate-spin configuration (21). This study is in progress and it will be reported in due course.

## ACKNOWLEDGMENTS

Financial support of UCM (Spain) through Research Project PR219/94-5570 and CICYT through Research Project MAT95-0642 are acknowledged. We are also grateful to Dr. S. Nicolopoulos for valuable technical assistance.

## REFERENCES

1. J. M. González-Calbet, M. Parras, J. M. Alonso, and M. Vallet-Regí, *J. Solid State Chem.* **106,** 99 (1993).
2. M. Parras, J. M. González-Calbet, J. A. Alonso, and M. Vallet-Regí, *J. Solid State Chem.* **113,** 78 (1994).
3. M. Parras, M. Vallet-Regí, J. M. González-Calbet, and J. C. Grenier, *J. Solid State Chem.* **83,** 121 (1989).
4. H. Taguchi, Y. Takeda, F. Kanamaru, M. Shimada, and M. Koizume, *Acta Crystallogr. Sect. B* **33,** 1299 (1977).
5. J. J. Lander, *Acta Crystallogr.* **4,** 148 (1951).
6. U. Spitsbergen, *Acta Crystallogr.* **13,** 197 (1960).
7. M. Zanne, A. Courtois, and C. Gleitzer, *Bull. Soc. Chim. Fr.* **12,** 4470 (1972).
8. A. J. Jacobson and J. L. Hutchison, *J. Solid State Chem.* **35,** 334 (1980).
9. M. Parras, A. Varela, H. Seehofer, and J. M. González-Calbet, *J. Solid State Chem.* **120,** 327 (1995).
10. K. R. Poeppelmeier, A. J. Jacobson, and J. M. Longo, *Mater. Res. Bull.* **15,** 339 (1980).
11. R. V. Shpanchenko, L. Nistor, G. Van Tendeloo, J. Van Landuyt, and S. Amelinckx, *J. Solid State Chem.* **114,** 560 (1995).
12. G. A. Candela, A. H. Kahn, and T. Negas, *J. Solid State Chem.* **7,** 360 (1973).
13. L. Barbey, N. Nguyen, V. Caignaert, M. Hervieu, and B. Raveau, *Mater. Res. Bull.* **27,** 295 (1992).
14. L. Barbey, N. Nguyen, V. Caignaert, F. Studer, and B. Raveau, *J. Solid State Chem.* **112,** 148 (1994).
15. Y. Minet, V. Lefranc, N. Nguyen, B. Domengès, A. Maignan, and B. Raveau, *J. Solid State Chem.* **121,** 158 (1996).
16. J. C. Grenier, L. Fournés, M. Pouchard, and P. Hagenmuller, *Mater. Res. Bull.* **21,** 441 (1986).
17. P. L. Gai, A. J. Jacobson, and C. N. R. Rao, *Inorg. Chem.* **15**(2), 480 (1976).
18. M. Parras, A. Varela, K. Boulahya, and J. M. González-Calbet, unpublished results.
19. J. DiCarlo, I. Yazdi, and A. J. Jacobson, *J. Solid State Chem.* **109,** 223 (1994).
20. R. D. Shannon, *Acta Crystallogr. Sect. A* **32,** 751 (1976).
21. G. Demazeau, M. Pouchard, M. Thomas, J. F. Colombet, J. C. Grenier, L. Fournes, J. L. Soubeyroux, and P. Hagenmuller, *Mater. Res. Bull.* **15,** 451 (1980).